Molecules and Cells

Research Article

Actin depolymerizing factor destrin governs cell migration in neural development during *Xenopus* embryogenesis

Youni Kim[1,5], Hyun-Kyung Lee[1,5], Kyeong-Yeon Park[1,5], Tayaba Ismail[1], Hongchan Lee[1], Hong-Yeoul Ryu[1], Dong-Hyung Cho[1], Taeg Kyu Kwon[2], Tae Joo Park[3], Taejoon Kwon[4], and Hyun-Shik Lee[1,*]

[1]KNU G-LAMP Project Group, KNU Institute of Basic Sciences, BK21 FOUR KNU Creative BioResearch Group, School of Life Sciences, College of Natural Sciences, Kyungpook National University, Daegu 41566, Korea, [2]Department of Immunology, School of Medicine, Keimyung University, Daegu 41566, Korea, [3]Department of Biological Sciences, College of Information-Bio Convergence, Ulsan National Institute of Science and Technology (UNIST), Ulsan 44919, Korea, [4]Department of Biomedical Engineering, College of Information-Bio Convergence, Ulsan National Institute of Science and Technology (UNIST), Ulsan 44919, Korea

[*]Corresponding author. leeh@knu.ac.kr
https://doi.org/10.1016/j.mocell.2024.100076

ABSTRACT

The actin-based cytoskeleton is considered a fundamental driving force for cell differentiation and development. Destrin (Dstn), a member of the actin-depolymerizing factor family, regulates actin dynamics by treadmilling actin filaments and increasing globular actin pools. However, the specific developmental roles of *dstn* have yet to be fully elucidated. Here, we investigated the physiological functions of *dstn* during early embryonic development using *Xenopus laevis* as an experimental model organism. *dstn* is expressed in anterior neural tissue and neural plate during *Xenopus* embryogenesis. Depleting *dstn* promoted morphants with short body axes and small heads. Moreover, *dstn* inhibition extended the neural plate region, impairing cell migration and distribution during neurulation. In addition to the neural plate, *dstn* knockdown perturbed neural crest cell migration. Our data suggest new insights for understanding the roles of actin dynamics in embryonic neural development, simultaneously presenting a new challenge for studying the complex networks governing cell migration involving actin dynamics.

Keywords: Destrin, F-actin, Neural crest, Neurulation, *Xenopus laevis*

INTRODUCTION

Actin filaments directly or indirectly participate in various cellular processes: Maintaining cell shape and polarity, migration, division, organelle transport, vesicle trafficking, axonal growth, muscle contraction, and phagocytosis (Svitkina, 2018; Winder and Ayscough, 2005). Moreover, participation largely depends on the assembly, disassembly, and treadmilling of actin filaments, termed “actin dynamics” (Bernstein and Bamburg, 2010). The family of actin-depolymerizing factors (ADFs) is primarily known as a regulator of actin dynamics, as they facilitate actin filament severing and depolymerization (Bamburg, 1999; Bamburg and O’Neil, 2002). The ADFs family members are evolutionarily conserved and are found in all eukaryotes (Maciver and Hussey, 2002). In addition, most mammals express 3 isoforms of ADF proteins, that is, destrin (DSTN, also known as ADF), cofilin-1 (CFL1), and cofilin-2 (CFL2). DSTN and CFL1 are most abundant in nonmuscle tissues, whereas CFL2 is predominantly expressed in muscles (Bamburg, 1999).

These dynamizing actin proteins play diverse roles in health and disease. Actin rod formation activity of ADFs engages in the occurrence of several neurodegenerative diseases in the early stages (Bernstein et al., 2006). Furthermore, it has been suggested that DSTN and CFL1 are involved in cytokinesis and gametogenesis, contributing to cancers and infertility in humans (Bamburg and O’Neil, 2002). CFL1 knockout mice are embryonic lethal at E11.5 to 12.5 and present defects in neural tube closure and neuronal cell migration, whereas DSTN knockout mice remain alive but exhibit abnormal cornea thickening, leading to postnatal blindness (Bellenchi et al., 2007; Ikeda et al., 2003; Tahtamouni et al., 2013). CFL1 appears essential for neuronal development and differentiation, but the DSTN requirement has yet to be studied. Thus, it is necessary to understand the developmental roles of DSTN to establish the exquisiteness of the ADF as an actin dynamics regulator in physiological processes.

Therefore, we investigated the developmental roles of *dstn* in embryogenesis, particularly during neurulation and neural crest development, using *Xenopus laevis*. We used the morpholino oligonucleotide (MO)-mediated knockdown of *dstn* in

[5] These authors contributed equally.

eISSN: 1016-8478

Xenopus-developing embryos. Our results indicated that *dstn* mediates the extension of the neural plate region by modulating actin dynamics, and *dstn* is involved in neural crest cell migration during *Xenopus* embryogenesis without affecting neural crest gene expression.

MATERIALS AND METHODS

Xenopus Maintenance and Embryo Manipulation

Adult *Xenopus laevis* were obtained from the Korean *Xenopus* Resource Center for Research and maintained in plastic aquarium tanks circulating dechlorinated water at 18 °C (recommended by the Institutional Review Board of Kyungpook National University, Korea). Ovulation was induced in *Xenopus* females by injecting 1,000 International units of human chorionic gonadotrophin, and eggs were fertilized *in vitro* and manipulated for further experiments, as described previously (Kim et al., 2018).

Experiments were strictly conducted according to the Animal Care and Use Committee guidelines, consistent with international laws and policies (National Institute of Health) Guide for the Care and Use of Laboratory Animals, publication no. 85-23, 1985). The Institutional Review Board of Kyungpook National University in Korea approved the experimental use of amphibians (2021-0017). All research group members were trained to care for and use experimental organisms appropriately.

Plasmid Construction, MO Design, and Microinjections

For messenger ribonucleic acid (mRNA) injection or *in situ* hybridization using RNA probes, *dstn* was designed based on National Center for Biotechnology Information and Xenbase sequences. For mRNA synthesis, plasmids were constructed using a pCS107 vector with restriction enzymes BamH1 and Xho1. The RNA probe sequence containing 200 to 300 base pairs of full-length genes was labeled with digoxigenin (DIG) and inserted into a T-easy vector (pGEM, Promega). Next, the pCS107 vectors and T-easy were linearized by Apa1, a restriction enzyme. Then, the capped mRNAs were synthesized using the SP6 mMessage mMachine kit (Invitrogen). Finally, DIG-labeling RNA probes were generated using the T7 mMessage mMachine kit (Invitrogen). The *dstn* MO is 25 nucleotides long and has the following base composition: 5′-TCCG AACACCTGATGCCATTGTTGA-3′. The control MO has the following sequence: 5′-CCTCTTACCTCAGTTACAATTTATA-3′. The MO was obtained from Gene Tools. For the rescue experiments, mutant constructs (*dstn**) not recognized by *dstn* MO were subcloned into the pCS107 vector using the abovementioned method. Finally, MOs and mRNAs were injected into the fertilized *Xenopus* embryos.

Whole-Mount In Situ Hybridization

Xenopus embryos were fixed in MEMFA (4% paraformaldehyde, 0.1 M (3-(N-morpholino) propanesulfonic acid) [pH 7.4], 1 mM $MgSO_4$, and 2 mM Ethylene glycol tetraacetic acid) at 4 °C overnight. The embryos were dehydrated before storage in 100% methanol at −20 °C, and whole-mount *in situ* hybridization (WISH) was performed as described previously (Kim et al., 2018). Probes were detected using an alkaline phosphatase-labeled anti-DIG antibody (1:1000, Roche) and Nitroblue tetrazolium dichloride/5-bromo-4-chloro-3-indolyl-phosphate staining solution (Roche).

Real-Time Quantitative Polymerase Chain Reaction

Total RNA was extracted from the *Xenopus* embryos, and complementary deoxyribonucleic acid was synthesized using the first strand complementary deoxyribonucleic acid synthesis kit (Takara). Furthermore, real-time quantitative polymerase chain reaction was performed with TB Green Premix Ex Taq (Takara) and specific primers (Table 1) using CFX Connect Real-Time PCR System (Bio-Rad).

Alcian Blue Staining

Xenopus embryos (NF. St. 49) were fixed in MEMFA and rehydrated in 50% Ethanol (EtOH). Then, the embryos were incubated in 0.04% Alcian blue (Sigma) staining solution (10 mM $MgCl_2$ and 80 % EtOH) for 3 days. Next, the stained embryos were bleached using a bleaching solution (3% H_2O_2, 5% formamide, 0.5× saline sodium citrate) and washed in 0.1× trypsin to dissolve soft tissue. Finally, embryos were transferred into buffered EtOH (0.25× saline sodium citrate, 75% EtOH) for storage.

Immunofluorescence and Confocal Microscopy

Xenopus embryos were fixed with MEMFA, and Alexa Fluor 488 phalloidin (1:1000, Invitrogen) was used to visualize F-actin. Image processing and analysis were performed using an Olympus FV1200 confocal microscope.

Western Blotting

Embryonic lysates were prepared from embryos using lysis buffer (137 mM NaCl, 20 mM Tris-HCl, 20 mM NP-40, 10% glycerol) with 1 mM phenylmethylsulfonyl fluoride, 5 mM sodium vanadate, and 1 mM protease inhibitor cocktail (Roche). The proteins were loaded and separated via 12% sodium dodecyl sulfate polyacrylamide gel electrophoresis and transferred to a nitrocellulose membrane. The membrane was blocked using a blocking solution (5% skim milk) at room temperature for 1 h. The proteins were detected with monoclonal anti-Flag antibody (1:1,000, Abcam) and monoclonal anti-beta actin (1:1,000, Santa Cruz). The secondary antibodies used were anti-mouse Immunoglobin G Horseradish peroxidase-linked antibodies (1:2,000, Santa Cruz).

Quantification and Statistics

Confocal and optical microscope imaging data were analyzed using ImageJ software (National Institutes of Health) and Zen software (Zeiss), respectively. Statistical analyses were performed using GraphPad (Dotmatics) Prism 7. The results are presented

Table 1. The primer sequences for real-time PCR

Gene	Forward primer	Reverse primer
odc	5’-GCTTCTGGAGCGGGCAAAGGA-3’	5’-CAACATGGAAACTCACACC-3′
dstn	5′- CGGGGGAAGCAACAAAACAG-3′	5′- CCCATTGCTTTTGGACACCTG-3′

as the mean ± standard deviation from at least 3 independent experiments (exact numbers are shown in graphs; *n*). The data were analyzed using Student's t-test, and the significance level was considered as $*P < .05$, $**P < .01$, $***P < .001$, $****P < .0001$.

RESULTS

dstn Is Expressed in Anterior Neural Tissue During *Xenopus* Embryogenesis

To better understand the developmental roles of *dstn*, we used real-time quantitative polymerase chain reaction to examine *dstn* expression at 9 landmark stages of *Xenopus* embryogenesis spanning blastula (Nieuwkoop and Farber stage 8; NF. St. 8), gastrula (NF. St. 12), neurula (NF. St. 16), early tailbud (NF. St. 22 and 26), and the late tailbud stage of development (NF. St. 32, 36, and 40) (Fig. 1A). Temporal expression data revealed that *dstn* was a maternal gene and expressed throughout each landmark stage of embryonic development (Fig. 1A). The tissue-specific expression of *dstn* analyzed by WISH was exhibited in neural tissues being localized in the anterior neural tissue, neural plate, eyes, branchial arch, and somites during the early tailbud development stages (NF. St. 16 and 22) (Fig. 1B). Furthermore, their expression, representing a dotted pattern, was detected in the *Xenopus* epithelium during the late tailbud development stage (NF. St. 32). The spatiotemporal expression pattern suggests that *dstn* has potential roles in neural tissue induction and neural crest development.

dstn Morphants Showed Phenotypic Abnormalities in the Malformed Body Axis and Small-Sized Head

To delineate the roles of *dstn* during *Xenopus* embryogenesis, we performed a loss of function study by microinjecting MOs targeting the *dstn* gene. Additionally, we designed an MO binding construct (*dstn* MOB) and rescue construct (*dstn**) that cannot bind with MO (Fig. 2A). The efficacy of *dstn* MO was analyzed using Western blotting. These results showed that *dstn* MOs effectively inhibited the translation of Flag-tagged *dstn* MOB mRNA constructs (Fig. 2B). However, this inhibition did not affect the Flag-tagged MO non-binding mRNA construct of *dstn* (*dstn**) in which MOB sites were mutated to prevent specific MOB (Fig. 2B). The control MO (40 ng) or *dstn* specific MO (40 ng) was injected into the 2-cell staged *Xenopus* embryos. The *dstn* morphants exhibited developmental abnormalities at late tailbud stages (NF. St. 31 and 41) compared with control MO-injected embryos. Most *dstn* knockdown embryos had small-sized heads, delayed eye development, bent tails, and shortened body axes (Fig. 2C). The delayed eye development in the knockdown embryos was recovered during the later stages of development. However, the small-sized heads persisted in the morphant embryos (NF. St. 47) (Fig. 2D). Thus, we performed Alcian blue staining to observe the effects of *dstn* on cartilage formation. Our results showed that the overall cartilage size was reduced in *dstn* morphants, but there were no structural anomalies observed in *dstn* knockdown embryos (Fig. 2D). Further, to verify that the developmental abnormalities were specifically induced by *dstn* depletion, rescue experiments were performed by microinjecting *dstn** mRNA with *dstn* MO. These results showed

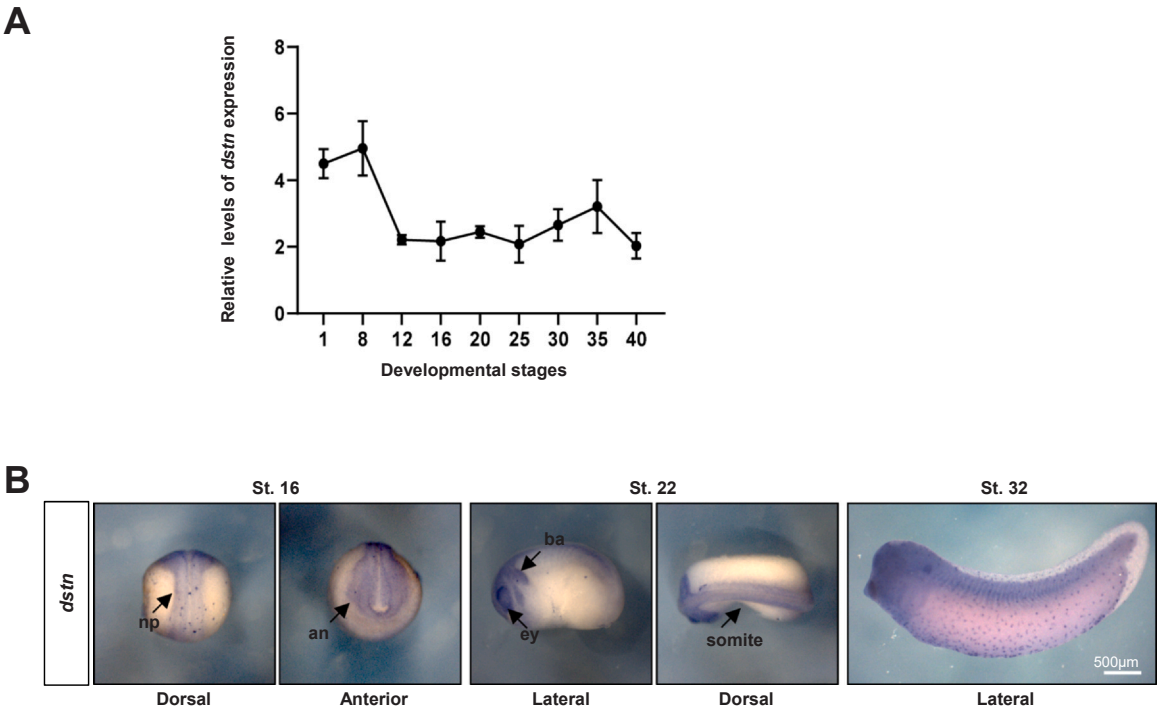

Fig. 1. *dstn* is expressed in anterior neural tissues and the epidermis during *Xenopus* embryogenesis. (A) Temporal expression of *dstn* analyzed by real-time qPCR at 9 landmark stages of embryonic development. (B) Spatial expression patterns of *dstn* were examined by whole-mount *in situ* hybridization (WISH). np, neural plate; an, anterior neural; ey, eye; ba, branchial arch; qPCR, quantitative polymerase chain reaction.

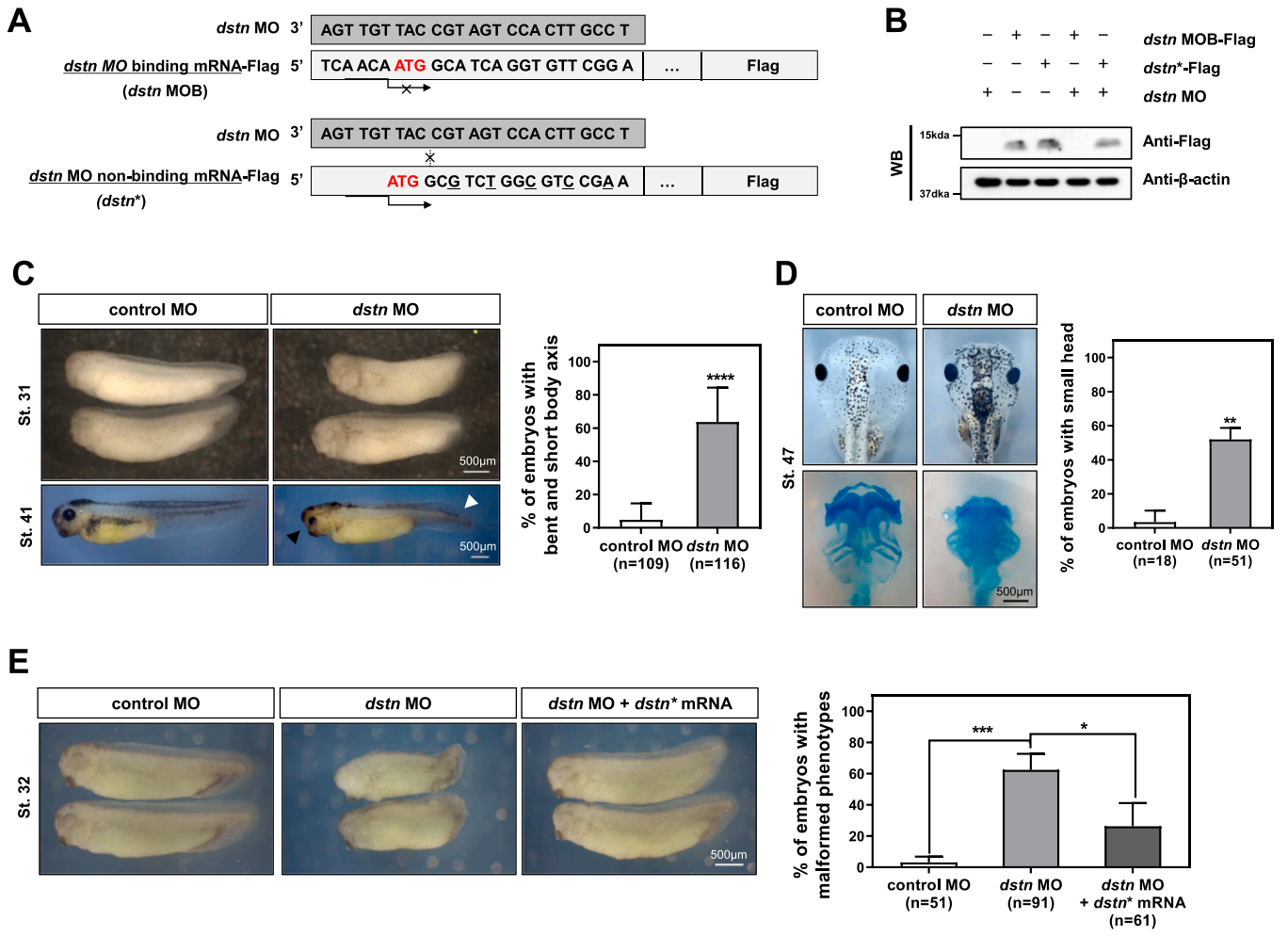

Fig. 2. *dstn* knockdown embryos show developmental malformations: short body axis and small-sized heads. (A) A graphical representation indicating *dstn* morpholino oligonucleotide (MO), *dstn* MO binding mRNA (*dstn* MOB)-Flag, *dstn* MO non-binding mRNA (*dstn**)-Flag construct that codes for destrin but possess a mutated 5′-UTR, which *dstn* MO cannot target. Co-delivery of the *dstn* MO and rescue mRNA produced the same phenotypes as wild-type *dstn* mRNA. (B) Western blotting confirmed the efficacy of *dstn* MO. Anti-β-actin was used as a loading control. (C) *dstn* MO (40 ng) was injected into the *Xenopus* embryos at the 2-cell stage, and the embryos were then fixed at developmental stages 31 and 41. White arrows represent the defects in tail development, and black arrows represent head and eye anomalies compared with control embryos. The statistical analysis showed that more than 60% of *dstn* morphants exhibited short and bent axes compared to control embryos. (D) Analysis of cartilage formation in *dstn* MO-injected embryos was conducted by fixing the embryos at stage 47, followed by staining with Alcian blue. The graphical representation indicated that more than 50% of *dstn* morphants showed small-sized heads compared to the control embryos. (E) Rescue experiments were performed by microinjecting the *dstn** mRNA with *dstn* MO at the 2-cell stage of embryos. The developing embryos fixed at stage 32 showed that the phenotypic malformations of the small-sized head and bent axis were effectively recovered by co-injecting the *dstn** and *dstn* MO. A graphical representation indicated that microinjection of *dstn** mRNA with *dstn* MO considerably rescued phenotypic malformations as observed in *dstn* morphants. The significance levels are shown as $*P < .05$, $**P < .01$, $***P < .001$, $****P < .0001$, ns, not significant.

that the embryos effectively recovered the developmental anomalies observed in *dstn* morphants (Fig. 2E). Collectively, our data suggest *dstn* is crucial for *Xenopus* embryogenesis.

Knockdown of *dstn* Impaired the Neural Plate Extension and Inhibited Cell Migration During *Xenopus* Embryogenesis

Considering the tissue-specific expression of *dstn* on the neural plate (Fig. 1B), we investigated the roles of *dstn* in neurulation during *Xenopus* development. To demonstrate the effect of *dstn* during neurulation, *dstn* MO was unilaterally microinjected into 1 blastomere of 2-cell staged *Xenopus* embryos, and the expression of neural plate marker *sox3* was observed. As shown in the neural plate marker, the *sox3* expression pattern resulted in a 20% wider neural plate on the MO-injected side of embryos compared with the MO-injected side of the control embryos (Fig. 3A). Furthermore, we cross-sectioned the embryos after *dstn* knockdown to observe the internal anatomy of neurula stage embryos (NF. St. 19). The gross internal structure showed a clear difference in distribution and position of mesodermal cells on the injected side (B) of the embryos compared with the uninjected side (A), although the notochord was formed normally in the control and

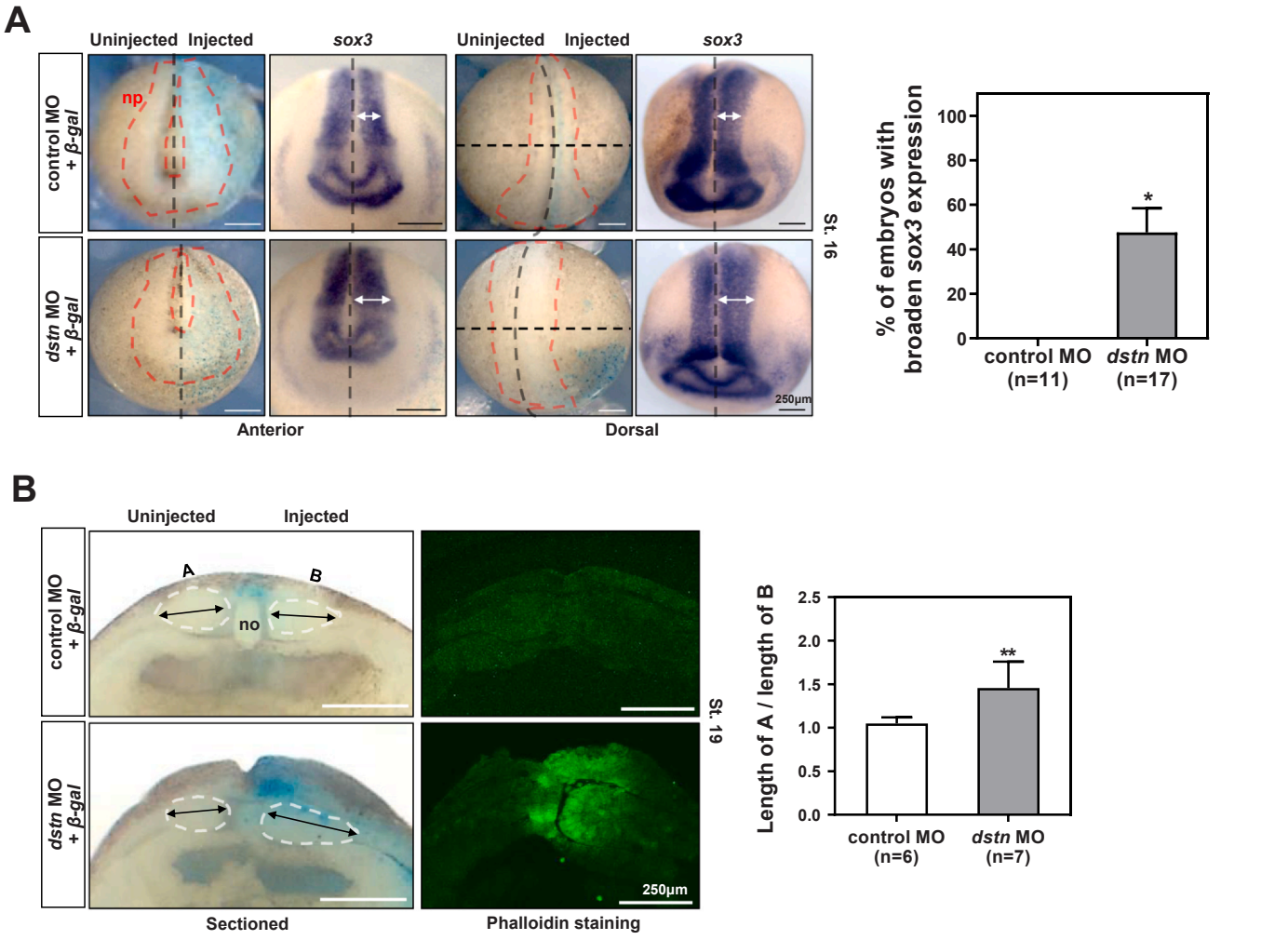

(caption on next page)

Fig. 3. *dstn* mediates neural plate extension and perturbs cell migration. (A) *dstn* MO was coinjected with *beta-galactosidase (β-gal*) mRNA into 1 blastomere of 2-cell staged embryos, and the embryos were then fixed at the late neurula stage (NF. St.16). β-gal staining indicated the injected side of the embryos. The length of the white-headed arrows exhibits the neural plate expansion in the *dstn* MO-injected side of the embryos compared to the shorter white-headed arrows in the control MO-injected side, as shown in the anterior and dorsal views. A graphical representation showed that approximately 50% of the *dstn* MO-injected embryos exhibited wider neural plates than the control embryos (scale bar: 250 μm). (B) Cross-sectional analysis of neurula stage embryos (NF. St.19) showed a difference in mesoderm distribution and position between the MO-injected side (B) and the uninjected side (A). Further, phalloidin immunostaining exhibited an accumulation of actin filaments (increased intensity) on the injected side of the embryos compared with the uninjected side. A graph representing the mean intensity of phalloidin staining showed a significant change in phalloidin intensity in *dstn* morphants compared to the control. Black arrows represent variation in the distribution and position of mesodermal cells (scale bar: 250 μm), no (notochord). (C) The *dstn* MO and *β-gal* mRNA microinjections indicated that cell migration was highly limited. Black arrows represent the reduced and restricted cell migration in dorsal (only dorsal view for early-stage embryos) and lateral views of developing embryos. Cell migration was restricted only to the head regions in the *dstn*-depleted embryos compared to cell migration from the head to the tail axis in control embryos. Statistical analysis of *dstn* morphants and control embryos revealed significant cell migration restriction in *dstn*-depleted embryos compared to control embryos (scale bar: 250 μm). $*P < .05$, $**P < .01$, $***P < .001$.

morphant embryos (Fig. 3B). The polymerization and depolymerization of actin filaments are important in neurulation (Schoenwolf et al., 1988; Ybot-Gonzalez and Copp, 1999). Since *dstn* plays a crucial role in regulating actin dynamics (Bamburg, 1999), we examined the effect of *dstn* inhibition on actin filaments during neurulation using fluorescent phalloidin that can effectively bind to actin filaments (Baldwin et al., 2022; Yamagishi and Abe, 2015). Confocal microscopy revealed the accumulation of actin filaments on the *dstn* MO-injected side of developing embryos (Fig. 3B) compared with evenly distributed filaments on the uninjected side and in control embryos.

Neurulation is a dynamic process that requires harmonized changes in cell shape and movements (Wallingford, 2005); furthermore, it depends on convergent extension and apical constriction (Copp et al., 2003; Wallingford, 2005). To elucidate whether *dstn*-suppression-induced neural plate extension depends on cell movements, we injected *dstn* MO with beta-galactosidase (*β-gal*) mRNA into the D.1.2 blastomere of developing embryos. The D.1.2 blastomere continues to divide and migrate throughout the spinal cord from head to tail and eventually differentiates according to the fate of each cell (Bauer et al., 1994; Moody, 1989). As shown in Figure 3C, *β-gal* staining at early (NF. St. 13) and later (NF. St. 32) stages of embryogenesis indicated cell movements. The dorsal view of embryos in the gastrula stage (NF. St. 13) indicated restricted cell movements after *dstn* depletion compared with control embryos (Fig. 3C). Moreover, unlike the expression of *β-gal* as observed in control embryos (from head to tail), the expression of *β-gal* was limited in head regions of *dstn* morphants (NF. St. 32), suggesting the involvement of *dstn* in cell migration (Fig. 3C). Altogether, our findings showed that the extended neural plate region observed in the *dstn* MO-injected side of the embryos exhibited an accumulation of actin filaments compared to the evenly distributed filaments in the uninjected side of the embryos and control MO-injected embryos. Owing to the accumulation of actin filaments, we speculated that the extension of the neural plate might involve actin filaments and interfere with restricted cell migration in *dstn* morphants.

dstn is Required for Neural Crest Migration During *Xenopus* Embryogenesis

Given the conflicting results between mouse studies showing that CFL1 is important for neurogenesis but DSTN can have different functions (Gurniak et al., 2005) and the study showing that DSTN can affect Neural crest migration in chicken models (Vermillion et al., 2014), the roles of DSTN during neural crest development should be further studied. We wondered whether *dstn* could regulate the expression of neural crest genes, which are crucial for early development. Neural crest cells are vertebrate stem cells that migrate and differentiate to generate various cell types throughout early development (Almeida et al., 2010). Hence, we performed WISH using neural crest markers, *snail2* and *sox9*. Following *dstn* depletion, *snail2* and *sox9* did not appear to be significantly affected, indicating that *dstn* does not affect neural crest specification (Fig. 4A). We discovered that *dstn* plays a role in cell migration during neurulation by affecting actin filament accumulation (Fig. 3) and these results raise the possibility that *dstn* may also be involved in neural crest migration. To examine the effect of *dstn* on neural crest migration, we performed WISH using embryos at stage 27 and the neural crest marker gene *twist*, which plays a role in the dissociation of neural crest cells by repressing E-cadherins in delaminating cells. Knockdown of *twist* led to upregulation of E-cadherins and inhibition of cell dispersion (Simões-Costa and Bronner, 2015). Our WISH *twist* data showed that *dstn* knockdown led to the downregulation of *twist* and inhibited neural crest migration. Therefore, our data indicate that *dstn* is not involved in neural crest specification but in migration.

DISCUSSION

Numerous independent studies have demonstrated cell-type-specific roles for DSTN and CFL1 in embryonic development (Gurniak et al., 2005; Hotulainen et al., 2005; Zhang et al., 2016). DSTN and CFL1 mutant mice showed the significance of CFL1 in neural crest migration and morphogenesis of neural tubes, whereas roles for DSTN during embryonic development were unappreciated (Gurniak et al., 2005). In previous studies, CFL1 was considered indispensable for cell migration, and DSTN-depleted chick cells revealed minor roles during neural crest migration (Vermillion et al., 2014). In contrast, DSTN and CFL1 exhibited overlapping roles in mammalian nonmuscle cells regulating actin dynamics (Hotulainen et al., 2005).

To understand the specific roles and detailed mechanisms of DSTN compared to CFL1 in embryonic development, we investigated the localization and expression pattern of *dstn* during *Xenopus laevis* embryogenesis. The maternal expression of *dstn* and its localization in anterior neural tissues, including neural plate, brain, and eyes (Fig. 1), implies it performs

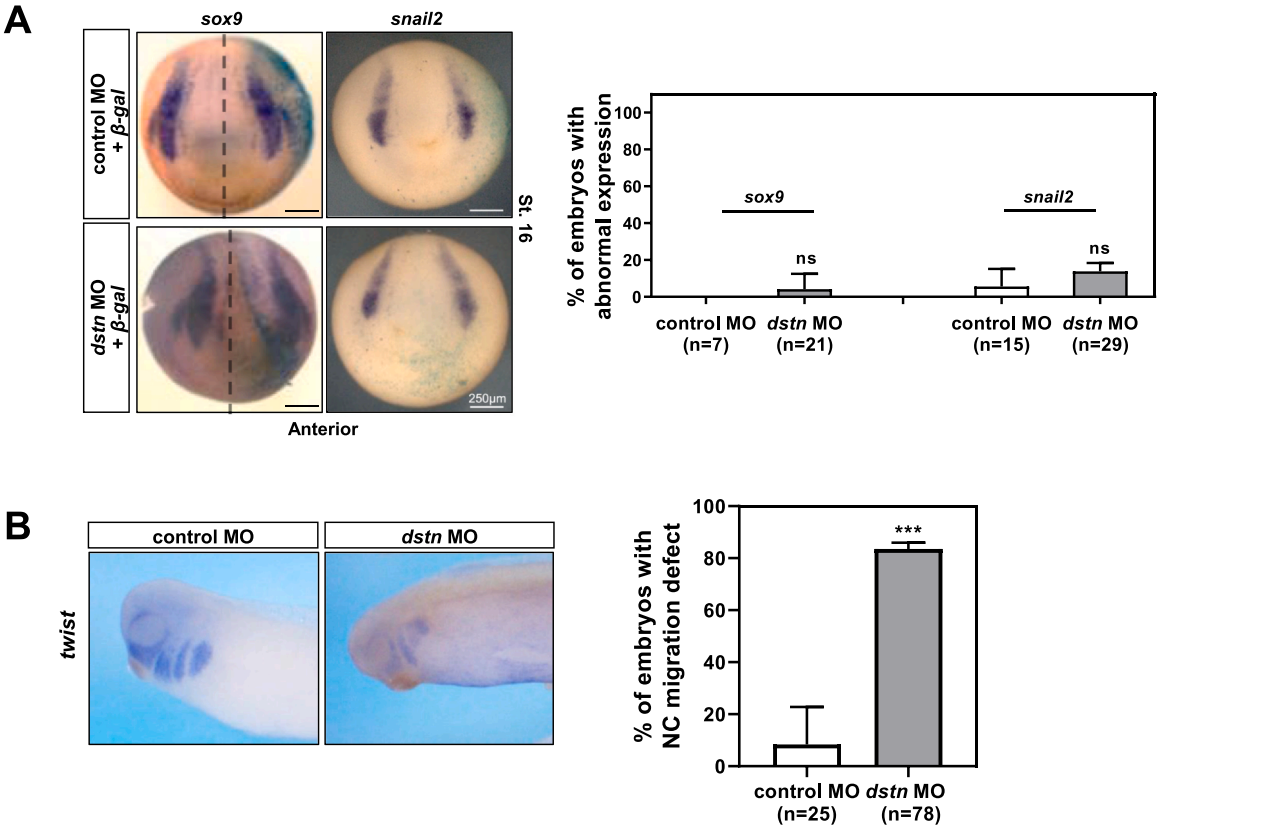

Fig. 4. *dstn* knockdown effects on neural crest specifiers during *Xenopus* embryogenesis. (A) Embryos were microinjected with *dstn* MO and *β-gal* mRNA and analyzed for neural crest-specific genes, *sox9,* and *snail2*. The uninjected side of the embryos served as an internal control. Statistical analysis showed no significant change in the expression of neural crest specifiers on the *dstn* MO-injected side of the embryos compared to the uninjected and control MO-injected sides (scale bar: 250 μm). (B) WISH analysis of *twist* in stage 27 embryos injected with control MO or *dstn* MO. Statistical analysis indicated that 80% of *dstn* morphants had defective neural crest migration compared to control MO-injected embryos (scale bar: 500 μm). nc, neural crest. ***$P < .001$, ns, not significant.

significant roles during *Xenopus* development. The loss of function study revealed that *dstn* deficiency induced developmental abnormalities, such as small-sized heads, delayed eye development, bent tails, and shortened body axes (Fig. 2). However, the delayed eye development was recovered during the later stages of embryonic development, although the smaller-sized head persisted throughout the last stage embryos (Fig. 2). The most plausible explanation for the delayed eye development at stage 41 and presentation of normal eyes at stage 47 is the regrowth ability of *Xenopus* eyes in embryos and tadpoles (Kha et al., 2018). *dstn* might affect the eye size at early development stages; meanwhile, *dstn* might not be involved in maintaining eye growth and size at later developmental stages. The smaller eyes observed during the early stages regained their normal size due to the regrowth ability of *Xenopus* eyes. However, regarding head size, *dstn* appeared to possess long-term effects that could not be recovered.

Additionally, our data present *dstn* roles during neurulation. The neural plate area labeled with *sox3* was expanded on the *dstn* MO-injected side of the embryos (Fig. 3A). Further, *sox3* overexpression is responsible for neural plate expansion by increasing cell proliferation (Archer et al., 2011). Conversely, *dstn* knockdown resulted in restricted migration of cells, meaning there might be a possibility that cell accumulation led to *sox3* overexpression, which ultimately resulted in the expansion of the neural plate—transverse histological sections of neural tissues at NF. St. 19 showed that the loss of *dstn* expanded the neural plate through an accumulation of F-actin. However, it did not affect neural tube formation (Fig. 3B). Likewise, the spatial expression of neural crest specifiers (*sox9* and *snail2*) was not affected by *dstn* depletion (Fig. 4A). Contrastingly, the expression of *twist* (neural crest specifier) was downregulated in *dstn* morphants (Fig. 4B). The contradictory expression of *sox9*, *snail2*, and *twist* in *dstn* morphants is possibly due to the roles of *sox9* and *snail2* in neural crest specifications since they act upstream of *twist.* In comparison, *twist* is a neural crest marker that plays a role in neural crest cell migration. Further, *twist* is involved in dissociating neural crest cells by repressing E-cadherins in delaminating cells. Thus, *twist* knockdown led to E-cadherins upregulation and cell dispersion inhibition (Simões-Costa and Bronner, 2015). Therefore, our results showed that *dstn* is required for neural crest cell migration but does not interfere with neural crest specification and differentiation.

Cell migration is a critical process in living organisms, and actin dynamics play a crucial role in regulating cell migration (Schaks et al., 2019). Thus, we conducted a migration assay using *β-gal* and WISH analyses of the neural crest marker, *twist*,

to determine the effect of *dstn* inhibition on cell migration during neurulation and neural crest development (Figs. 3C and 4B). These results demonstrate that *dstn,* a key ADF, modulates cell migration during embryogenesis in neural and neural crest development. Our data expand upon the previous results in mouse and chick cells, revealing the vital and independent roles of *dstn* during cell migration.

Additional pioneering studies have also shown the involvement of DSTN and CFL1 in neurodegenerative disorders, such as Alzheimer's, by promoting the formation of hyperphosphorylated Tau and amyloid beta (Bamburg et al., 2010; Kang and Woo, 2019; Rush et al., 2018). Our data provided convincing evidence that small-sized heads and expanded neural plates in *dstn* morphants indicate the involvement of ADFs with neurodegenerative disorders.

In conclusion, by regulating cell migration, *dstn* plays a significant role during *Xenopus* embryogenesis, particularly in neurulation and neural crest development. Thus, our study suggests new insights for understanding the roles of actin dynamics in embryonic development.

AUTHOR CONTRIBUTIONS

Youni Kim, Hyun Kyung Lee, and Kyeong-Yeon Park performed the experiments; Youni Kim, Tayaba Ismail, Hongchan Lee, and Hyun-Shik Lee performed data analysis and wrote the manuscript. Hyun Kyung Lee, Tayaba Ismail, HongYeol Ryu, and Dong-Hyung Cho reviewed and edited the manuscript. Taeg Kyu Kwon, Tae Joo Park, Taejoon Kwon, and Hyun-Shik Lee designed experiments, interpreted the results. Hong Yeol Ryu, Dong-Hyung Cho, and Hyun-Shik Lee critically analysed the manuscript and funding acquisition is provided by Hyun-Shik Lee. All the authors read and approved the final manuscript.

DECLARATION OF COMPETING INTERESTS

The authors declare that they have no known competing financial interests or personal relationships that could have appeared to influence the work reported in this paper.

ACKNOWLEDGMENTS

This work was supported by the Korea Environment & Technology Institute (KEITI) through the Core Technology Development Project for Environmental Diseases Prevention and Management, which was funded by the Korea Ministry of Environment (MOE) (grant number 2022003310001) and the National Research Foundation of Korea and the Ministry of Science & ICT (grant number 2021R1A2C1010408).

ORCID

Youni Kim: https://orcid.org/0000-0002-3052-6754
Hyun-Kyung Lee: https://orcid.org/0000-0003-4989-698X
Kyeong-Yeon Park: https://orcid.org/0009-0009-2509-9047
Tayaba Ismail: https://orcid.org/0000-0001-9970-4793
Hongchan Lee: https://orcid.org/0000-0001-9009-209X
Hong Yeoul Ryu: https://orcid.org/0000-0002-3367-9887
Dong-Hyung Cho: https://orcid.org/0000-0002-8859-0310
Taeg Kyu Kwon: https://orcid.org/0000-0003-1204-2059
Tae Joo Park: https://orcid.org/0000-0003-3176-177X
Taejoon Kwon: https://orcid.org/0000-0002-9794-6112
Hyun-Shik Lee: https://orcid.org/0000-0002-3837-9867

Received March 5, 2024
Revised May 13, 2024
Accepted May 27, 2024
Available online 31 May 2024.

REFERENCES

Almeida, A.D., Wise, H.M., Hindley, C.J., Slevin, M.K., Hartley, R.S., and Philpott, A. (2010). The F-box protein Cdc4/Fbxw7 is a novel regulator of neural crest development in *Xenopus laevis*. Neural Dev. *5*, 1-20.

Archer, T.C., Jin, J., and Casey, E.S. (2011). Interaction of Sox1, Sox2, Sox3 and Oct4 during primary neurogenesis. Dev. Biol. *350*, 429-440.

Baldwin, A.T., Popov, I.K., Wallingford, J.B., and Chang, C. (2022). Assays for apical constriction using the *Xenopus* model. Methods Mol. Biol. *2438*, 415-437.

Bamburg, J.R. (1999). Proteins of the ADF/cofilin family: essential regulators of actin dynamics. Annu. Rev. Cell Dev. Biol. *15*, 185-230.

Bamburg, J.R., Bernstein, B.W., Davis, R.C., Flynn, K.C., Goldsbury, C., Jensen, J.R., Maloney, M.T., Marsden, I.T., Minamide, L.S., Pak, C.W., et al. (2010). ADF/Cofilin-actin rods in neurodegenerative diseases. Curr. Alzheimer Res. *7*, 241-250.

Bamburg, J.R., and O'Neil, P.W. (2002). ADF/cofilin and actin dynamics in disease. Trends Cell Biol. *12*, 598-605.

Bauer, D.V., Huang, S., and Moody, S.A. (1994). The cleavage stage origin of Spemann's Organizer: analysis of the movements of blastomere clones before and during gastrulation in *Xenopus*. Development, *120*, 1179-1189.

Bellenchi, G.C., Gurniak, C.B., Perlas, E., Middei, S., Ammassari-Teule, M., and Witke, W. (2007). N-cofilin is associated with neuronal migration disorders and cell cycle control in the cerebral cortex. Genes Dev. *21*, 2347-2357.

Bernstein, B.W., and Bamburg, J.R. (2010). ADF/cofilin: a functional node in cell biology. Trends Cell Biol. *20*, 187-195.

Bernstein, B.W., Chen, H., Boyle, J.A., and Bamburg, J.R. (2006). Formation of actin-ADF/cofilin rods transiently retards decline of mitochondrial potential and ATP in stressed neurons. Am. J. Physiol.-Cell Physiol. *291*, C828-C839.

Copp, A.J., Greene, N.D., and Murdoch, J.N. (2003). The genetic basis of mammalian neurulation. Nat. Rev. Genet. *4*, 784-793.

Gurniak, C.B., Perlas, E., and Witke, W. (2005). The actin depolymerizing factor n-cofilin is essential for neural tube morphogenesis and neural crest cell migration. Dev. Biol. *278*, 231-241.

Hotulainen, P., Paunola, E., Vartiainen, M.K., and Lappalainen, P. (2005). Actin-depolymerizing factor and cofilin-1 play overlapping roles in promoting rapid F-actin depolymerization in mammalian nonmuscle cells. Mol. Biol. Cell, *16*, 649-664.

Ikeda, S., Cunningham, L.A., Boggess, D., Hobson, C.D., Sundberg, J.P., Naggert, J.K., Smith, R.S., and Nishina, P.M. (2003). Aberrant actin cytoskeleton leads to accelerated proliferation of corneal epithelial cells in mice deficient for destrin (actin depolymerizing factor). Hum. Mol. Genet. *12*, 1029-1036.

Kang, D.E., and Woo, J.A. (2019). Cofilin, a master node regulating cytoskeletal pathogenesis in Alzheimer's disease. J. Alzheimers Dis. *72*, S131-S144.

Kha, C.X., Son, P.H., Lauper, J., and Tseng, K.A.-S. (2018). A model for investigating developmental eye repair in *Xenopus laevis*. Exp. Eye Res. *169*, 38-47.

Kim, Y., Jeong, Y., Kwon, K., Ismail, T., Lee, H.-K., Kim, C., Park, J.-W., Kwon, O.-S., Kang, B.-S., Lee, D.-S., et al. (2018). Physiological effects of KDM5C on neural crest migration and eye formation during vertebrate development. Epigenet. Chromatin, *11*, 72.

Maciver, S.K., and Hussey, P.J. (2002). The ADF/cofilin family: actin-remodeling proteins. Genome Biol. *3*, 1-12.

Moody, S.A. (1989). Quantitative lineage analysis of the origin of frog primary motor and sensory neurons from cleavage stage blastomeres. J. Neurosci. *9*, 2919-2930.

Rush, T., Martinez-Hernandez, J., Dollmeyer, M., Frandemiche, M.L., Borel, E., Boisseau, S., Jacquier-Sarlin, M., and Buisson, A. (2018). Synaptotoxicity in Alzheimer's disease involved a dysregulation of actin cytoskeleton dynamics through cofilin 1 phosphorylation. J. Neurosci. *38*, 10349-10361.

Schaks, M., Giannone, G., and Rottner, K. (2019). Actin dynamics in cell migration. Essays Biochem. *63*, 483-495.

Schoenwolf, G.C., Folsom, D., and Moe, A. (1988). A reexamination of the role of microfilaments in neurulation in the chick embryo. Anat. Record, *220*, 87-102.

Simões-Costa, M., and Bronner, M.E. (2015). Establishing neural crest identity: a gene regulatory recipe. Development, *142*, 242-257.

Svitkina, T. (2018 Jan 2). The actin cytoskeleton and actin-based motility. Cold Spring Harb. Perspect. Biol. *10*(1), a018267. https://doi.org/10.1101/cshperspect.a018267 PMID: 29295889; PMCID: PMC5749151.

Tahtamouni, L.H., Shaw, A.E., Hasan, M.H., Yasin, S.R., and Bamburg, J.R. (2013). Non-overlapping activities of ADF and cofilin-1 during the migration of metastatic breast tumor cells. BMC Cell Biol. *14*, 45.

Vermillion, K.L., Lidberg, K.A., and Gammill, L.S. (2014). Expression of actin-binding proteins and requirement for actin-depolymerizing factor in chick neural crest cells. Dev. Dyn. *243*, 730-738.

Wallingford, J.B. (2005 May 15). Neural tube closure and neural tube defects: studies in animal models reveal known knowns and known unknowns. Am J Med Genet C Semin Med Genet, *135C*(1), 59-68. https://doi.org/10.1002/ajmg.c.30054 PMID: 15806594.

Winder, S.J., and Ayscough, K.R. (2005). Actin-binding proteins. J. Cell Sci. *118*, 651-654.

Yamagishi, Y., and Abe, H. (2015). Reorganization of actin filaments by ADF/cofilin is involved in formation of microtubule structures during Xenopus oocyte maturation. Mol. Biol. Cell, *26*, 4387-4400.

Ybot-Gonzalez, P., and Copp, A.J. (1999). Bending of the neural plate during mouse spinal neurulation is independent of actin microfilaments. Dev. Dyn.: Off. Publ. Am. Assoc. Anat. *215*, 273-283.

Zhang, C., Zhang, W., Lu, Y., Yan, X., Yan, X., Zhu, X., Liu, W., Yang, Y., and Zhou, T. (2016). NudC regulates actin dynamics and ciliogenesis by stabilizing cofilin 1. Cell Res. *26*, 239-253.